

Josephson Current Counterflow in Atomic Bose-Einstein Condensates

E. Sakellari, N. P. Proukakis, M. Leadbeater, and C. S. Adams

Department of Physics, University of Durham, Durham DH1 3LE, United Kingdom

Abstract.

Josephson weak links in superconductors can be engineered such that the phase difference across the junction is π (π -junction), leading to the reversal of the current. The conditions under which the analogous effect of supercurrent counterflow can be achieved in a double-well atomic Bose-Einstein condensate are investigated. It is shown that this effect is observable for condensates of up to a few thousand atoms, which are initially prepared in an anti-symmetric ' π -state' and subsequently subjected to a uniformly increasing magnetic field gradient. This effect is found to be only weakly-dependent on trap geometry, and can be observed in both attractive and repulsive condensates.

Note: A substantially revised version of this manuscript (with various figures removed, improved discussion and some additional material) is available on [cond-mat/0312396](https://arxiv.org/abs/cond-mat/0312396).

1. Introduction

The creation of superconducting [1] and superfluid [2] weak links has led to the experimental observation of Josephson effects [3], arising as a result of macroscopic quantum phase coherence. Josephson weak links are typically created by connecting two initially independent systems (superconductors / superfluids) via a barrier with dimensions of the order of the system healing length. Such junctions lead to a variety of interesting phenomena [4], such as dc- and ac-Josephson effects, Shapiro resonances, macroscopic quantum self-trapping and π -phase oscillations. Observations in superconductors preceded those in superfluids, due to the much larger healing lengths, thus enabling easier fabrication of weak links. Evidence for Josephson-like effects has been observed in ^4He weak links [5], and unequivocally demonstrated for weakly-coupled ^3He systems [6]. The recent achievement of dilute trapped atomic Bose-Einstein condensation (BEC) [7] gives rise to a new system for studying Josephson effects. In particular, such systems enable the investigation of dynamical regimes not easily accessible with other superconducting or superfluid systems. The simplest atomic Josephson junction can be realized by a condensate confined in a double-well potential. To allow control of the tunnelling rate, such a system can be constructed by raising a barrier within a harmonic trap containing an atomic condensate; this can be achieved by the application of a far-off-resonant blue-detuned laser beam, which induces a repulsive gaussian barrier [8]. Atomic interferometry based on such a set-up was recently reported [9]. Alternatively, a condensate can be created directly in a magnetic double-well structure [10]. Remarkable experimental progress has led to the creation of atomic BEC Josephson junction arrays, in which the harmonically trapped atoms are additionally confined by an optical lattice potential, generated by far-detuned laser beams. Phase coherence in different wells was observed by interference experiments of condensates released from the lattice [11]. In addition, Josephson effects [12] and the control of tunnelling rate has been demonstrated [14, 13]. Although experiments (and theoretical analysis) of such systems are well underway, deeper insight into the diverse range of Josephson phenomena can be obtained by looking at the simplest single junction, double-well system. This system has already received considerable theoretical attention, with treatments based on a two-state approximation [15, 16, 17, 18, 19, 20, 21], zero temperature mean field theory [22, 23, 25, 26, 24, 27], quantum phase models [28, 29] and instanton methods [30].

This paper focuses on a double-well atomic BEC, and investigates the conditions under which the Josephson current can be engineered to flow in a direction opposite to that minimizing the potential energy. This phenomenon bears close analogies to superconducting π -junctions [31], in which a macroscopic phase difference $\phi = \pi$ is maintained across the superconducting weak link. Such behaviour has been observed in a variety of systems, as a consequence of different microscopic mechanisms. For example, π -junctions in ceramic superconductors have their origin in the symmetry of the order parameter [32], with their experimental detection being central to the understanding

of high- T_c superconductivity. π -junctions can also be created in ferromagnetic weak links [33], or by magnetic impurities [34]. Recent interest has focused on the creation of controllable π -junctions in superconducting/normal-metal/superconducting links, in which the current direction can be reversed by the application of suitably large voltage across the link [35]. The reversal originates from the fact that the addition of an extra phase factor π is equivalent to reversing the sign of the current I_c , since the superflow current obeys $I = I_c \sin(\phi)$. A controllable π -SQUID (Superconducting Quantum Interference Device) has been demonstrated [36], and it is clear that the manipulation of multiple such π -junctions will be important in the domain of quantum electronics. For example, an array of alternating $0 - \pi$ junctions allows the spontaneous generation of half-integer flux quanta. Such a circuit of multiple successive $0 - \pi$ junctions has been recently created between thin films of high- T_c and low- T_c superconductors [37], generating a one-dimensional array of Josephson contacts with alternating signs of current. The superfluid analogue of a superconducting π -junction is a metastable π -state. This was recently observed in ^3He weak links [38] upon exciting the system by an oscillating driving force. Atomic BEC junctions behave similarly to those of ^3He . For example, in the usual manner of considering mechanical analogs of Josephson junctions, superconducting Josephson junctions can be mapped onto a rigid pendulum, whereas atomic tunnel junctions (^3He , BEC) map onto a non-rigid pendulum [39], thus exhibiting richer oscillation modes. This model has been used to discuss so-called π oscillations [40] and their stability in atomic BEC's [41], while such states have also been shown to arise within the framework of an exact quantum phase model [29].

In this paper, we investigate the circumstances under which one can reverse the direction of the atomic current across a suitably-prepared condensate-condensate weak link, by the application of a linear potential gradient. We find that a BEC confined in a double well configuration can, for small values of the potential gradient, move towards the higher potential well, a phenomenon henceforth referred to as Josephson counterflow. Although such Josephson counterflow bears close analogies to the behaviour observed in superconducting weak links, we should point out that the counterflow discussed in this paper is 'global' (i.e. flow of entire quantum gas in opposite direction), as opposed to 'local' counterflow (i.e. across a single junction) in a superconducting $0 - \pi$ junction.

This paper discusses in detail the phenomenon of Josephson counterflow for the lowest state exhibiting such behaviour, namely the anti-symmetric first excited π -state, which is most amenable to experimental observation. Atomic counterflow dynamics are investigated in terms of experimentally relevant parameters, such as interaction strength, harmonic trap aspect ratio and gaussian barrier geometry. Our analysis is based on numerical simulations of the Gross-Pitaevskii equation in three dimensions and leads to the conclusion that there exists a realistic window of parameters in which atomic Josephson counterflow can be experimentally observed. This effect is found to be only weakly dependent on the strength of the interactions and can, in principle, be observed for both attractive and repulsive condensates. One should note the distinction between the π -state considered in this paper which is a time-independent solution, as

opposed to the π oscillations which arise as a result of a superposition of ground and first excited states. In an experimental realization, it may be difficult to create a pure π -state, and the system may experience a combination of counterflow and π -oscillations. In this paper we show that, by careful initial state preparation, one can decouple the timescales for these two effects, and even induce counterflow in a direction opposite to that of π -oscillations, thus demonstrating the different origin of these two phenomena. Note that Josephson counterflow has already been predicted in condensates trapped in optical lattices, as a result of the renormalization of the mass in the lattice, based on Bloch wave analysis [42]. Such an interpretation is, however, not easily transferable to the double-well system.

This paper is structured as follows. Sec. 2 introduces our main formalism, outlining the behaviour of a double-well condensate. Sec. 3 discusses the dynamics of atomic Josephson junctions, whereas the possibility of experimental observation of this phenomenon in current BEC set-ups is analysed in Sec. 4; finally, we conclude in Sec. 5.

2. BEC in a double-well potential

At low temperatures, the behaviour of a Bose-Einstein condensate is accurately described by a nonlinear Schrödinger equation known as the Gross-Pitaevskii (GP) equation. Throughout this paper we work in dimensionless (harmonic oscillator) units, by applying the following scalings: space coordinates transform according to $\mathbf{r}'_i = a_\perp^{-1} \mathbf{r}_i$, time $t' = \omega_\perp t$, condensate wavefunction $\psi'(\mathbf{r}', t') = \sqrt{a_\perp^3} \psi(\mathbf{r}, t)$ and energy $E' = (\hbar\omega_\perp)^{-1} E$. Here $a_\perp = \sqrt{\hbar/m\omega_\perp}$ is the harmonic oscillator length in the transverse direction(s), where ω_\perp the corresponding trapping frequency. We thus obtain the following dimensionless GP equation (primes henceforth neglected for convenience) describing the evolution of the condensate wavefunction (normalised to unity)

$$i\partial_t \psi(\mathbf{r}, t) = \left[-\frac{1}{2} \nabla^2 + V(\mathbf{r}) + \tilde{g} |\psi(\mathbf{r}, t)|^2 \right] \psi(\mathbf{r}, t). \quad (1)$$

The atom-atom interaction is parametrized by $\tilde{g} = g/(a_\perp^3 \hbar\omega_\perp)$, where $g = \mathcal{N}(4\pi\hbar^2 a/m)$ is the usual three-dimensional scattering amplitude, defined in terms of the s -wave scattering length a , and \mathcal{N} is the total number of atoms (mass m). $V(\mathbf{r})$ represents the total confining potential. Steady state solutions of the GP equations can be obtained by substituting $\psi(\mathbf{r}, t) = e^{-i\mu t} \phi(\mathbf{r})$.

In the double-well configuration, the total confining potential is given by (see Fig. 1(a))

$$V(\mathbf{r}) = \frac{1}{2} [(x^2 + y^2) + \lambda^2 z^2] + h \exp[-(z/w)^2] + \Delta z. \quad (2)$$

The first term describes a cylindrically symmetric harmonic trapping potential, with a trap aspect ratio $\lambda = \omega_z/\omega_\perp$: the trap is spherical for $\lambda = 1$, 'cigar-shaped' for $\lambda < 1$ and 'pancake-like' for $\lambda > 1$. The second term describes a gaussian potential of height h generated by a blue detuned light sheet of beam waist w in the z direction, located at

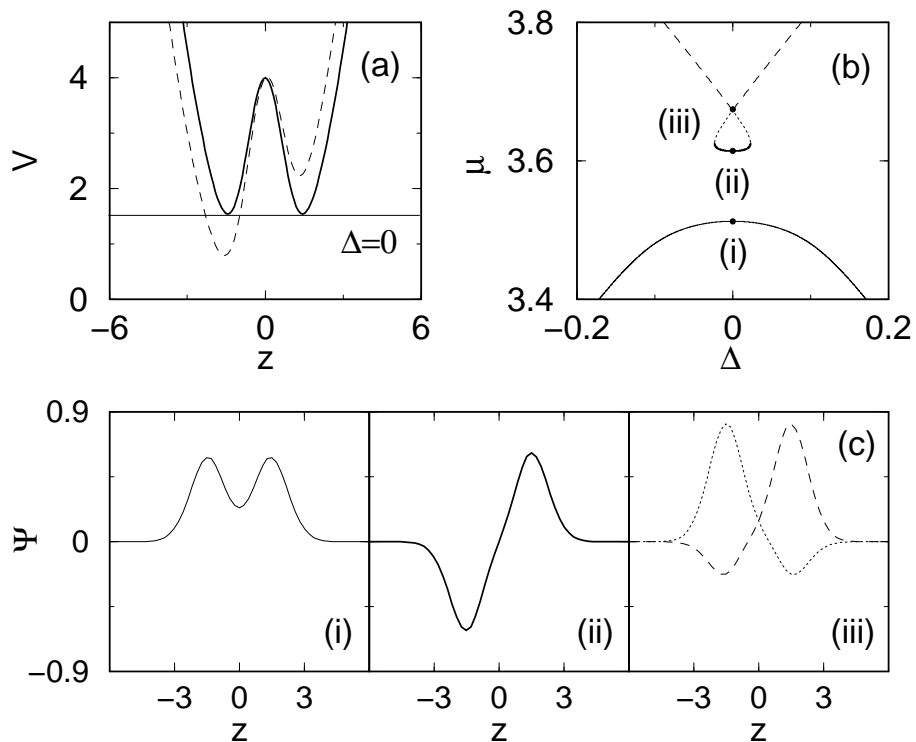


Figure 1. Double well potential with corresponding eigenenergies and eigenstates. (a) Schematic geometry of the total confining potential in the axial direction for a Gaussian barrier (height $h = 4\hbar\omega_{\perp}$, waist $w = a_{\perp}$) located at the centre of the trap. Plotted are the symmetric ($\Delta = 0$, solid line) and asymmetric ($\Delta = 0.5(\hbar\omega_{\perp}/a_{\perp})$, dashed line) case. (b)-(c) Corresponding eigenenergies and eigenstates for the double-well as a function of the potential gradient Δ : (i) ground state (lower thin solid line), (ii) anti-symmetric first-excited π -state (thick solid line), (iii) first excited state with unequal populations, having more population in left well (dotted), or in right well (dashed). Parameters used here are $\tilde{g} = \pi$ and spherical trap geometry ($\lambda = 1$).

$z = 0$. Finally, the contribution Δz corresponds to a linear magnetic field gradient Δ pivoted at the centre of the trap. The populations of the two wells are equal for $\Delta = 0$ (symmetric case, solid line in Fig. 1(a)), whereas $\Delta > 0$ (dashed line in Fig. 1(a)) leads to a tilted potential, which induces tunnelling. The application of the magnetic field gradient $\Delta > 0$ additionally shifts the trap centre to the $z > 0$ region. However, this shift is negligible for the parameters studied throughout this work, and will be henceforth ignored.

The eigenenergy curves of the double-well condensate are calculated by numerical solution of the time-independent GP equation, as discussed in more detail in our preceding paper [27]. Sufficiently large interactions lead to the appearance of a loop structure [20, 43]. The loop structure for the first excited state is shown in Fig. 1(b). Corresponding wavefunctions for ground (solid) and first excited state (dashed) are shown in Fig. 1(c) for $\Delta = 0$. The three eigenstates are (i) a symmetric state with equal population in both wells (solid line), (ii) an anti-symmetric ‘ π -state’ with equal

population in both wells and a phase difference of π across the trap centre, and (iii) two higher energy ‘self-trapped’ states with most of the population in either the left (dashed) or the right (dotted) well.

In this paper, we are mostly interested in the behaviour of the π -state. We will show that, if the system is prepared in the π state, the subsequent temporal evolution of the system can exhibit Josephson counterflow.

3. Josephson Counterflow Dynamics

To demonstrate counterflow, we study Josephson dynamics of the π -state under a potential gradient $\Delta > 0$, which is linearly increasing at rate R (i.e. $\Delta = Rt$), such that the right well lies higher than the left well (dashed line in Fig. 1(a)). On the basis of the usual Josephson relations, one might naively expect the atomic current to flow towards the region of lower potential, i.e. towards the left well. Instead, we observe that, for suitable parameters (see later), superflow can occur from the lower potential energy well (left) to the higher potential energy one (right). This is a direct consequence of the π phase difference of the antisymmetric initial wavefunction, and does not occur for a system in the symmetric ground state (for which flow always occurs

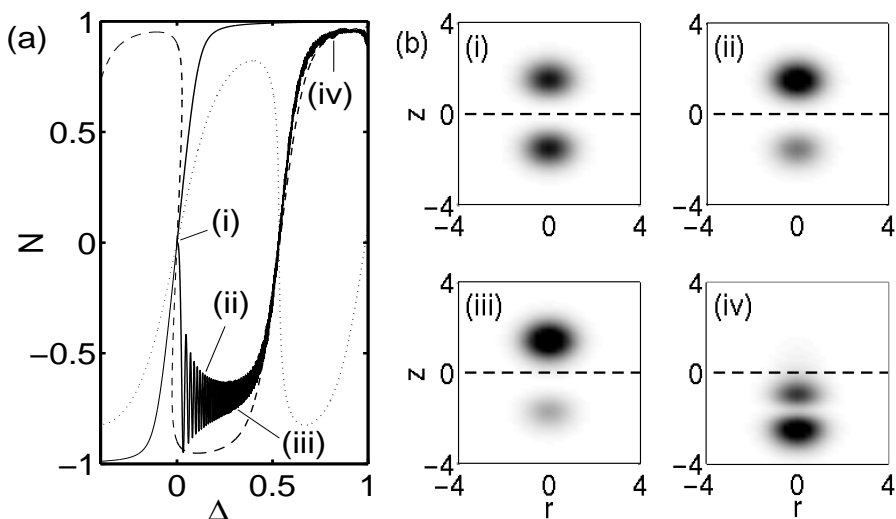


Figure 2. (a) Evolution of fractional population difference N as a function of potential gradient Δ , for a system initially prepared in a π -state. Here $h = 4\hbar\omega_{\perp}$, $\lambda = 1$, $\tilde{g} = \pi$ and the potential gradient $\Delta = Rt$ increases at constant rate $R = 10^{-3}(\hbar\omega_{\perp}^2/a_{\perp})$. The corresponding population differences for the ground state (thin solid), first excited (dashed) and second excited state (dotted) eigenstates are also shown. (b) Snapshots of the evolution of the density distribution for case (a) when (i) $\Delta = 0$, (ii) 0.1, (iii) 0.3 and (iv) 0.8 in units of $(\hbar\omega_{\perp}/a_{\perp})$. The population of both wells is initially equal ($\Delta = 0$). As the gradient is increased in (ii), (iii), population starts being transferred towards the right ($z > 0$), upper well. Increasing the asymmetry beyond a threshold value leads the population to be once again transferred to the left ($z < 0$), lower well. Eventually, (iv), a transition to the second excited state occurs (d) (see movie).

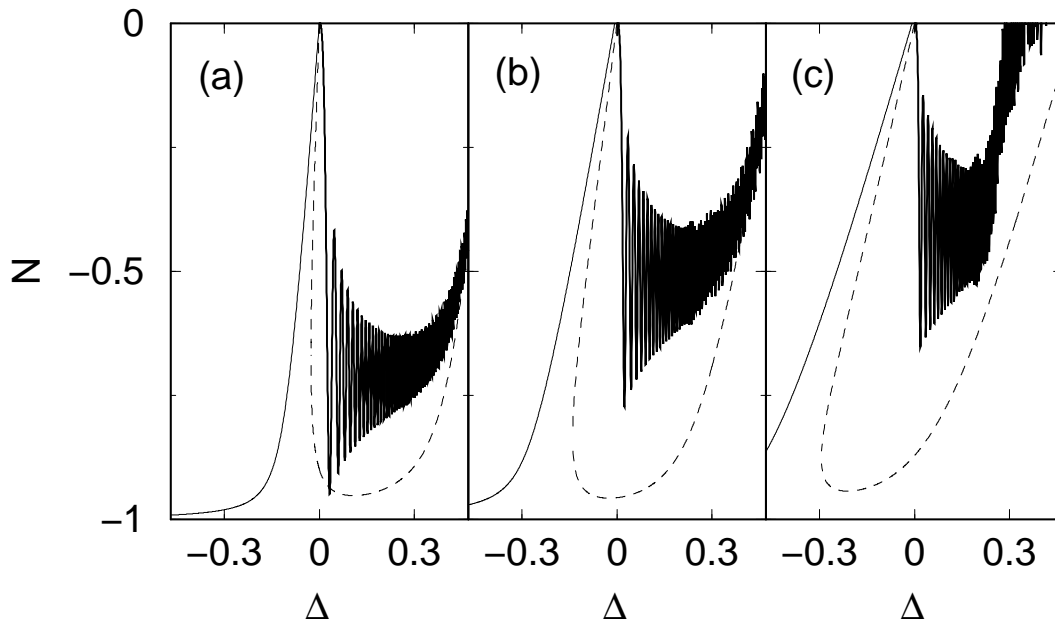


Figure 3. Evolution of fractional population difference N as a function of potential gradient Δ for identical trap configurations ($\lambda = 1$, $h = 4\hbar\omega_{\perp}$ and $R = 10^{-3}(\hbar\omega_{\perp}^2/a_{\perp})$) and increasing nonlinearity (a) $\tilde{g} = \pi$, (b) 4π and (c) 10π . Solid bold (dashed) lines indicate corresponding eigenstate populations for the ground (first excited) state.

towards regions of lower potential energy - see, e.g. [27]). Our study focuses on the dynamics of the fractional relative population, $N = (N_L - N_R)/(N_L + N_R)$, between the two wells, as opposed to the current through the junction (which is the derivative of N). The dependence of N on potential gradient Δ is shown for a spherical trap in Fig. 2(a), for a system initially prepared in the π -state. In such a state, the population of both wells is initially equal ($\Delta = 0$). As the gradient is increased, population starts being transferred towards the right, upper well, such that we observe Josephson counterflow to regions of higher potential energy. However, increasing the gradient beyond a threshold value leads to suppression of this effect, with the population once again transferred to the left, lower well. Eventually, the perturbation due to the applied potential becomes so pronounced, that a transition to the second excited state occurs [27]. Characteristic density snapshots of this evolution are shown in Fig. 2(b). The initial counterflow dynamics can be understood by means of lowest order perturbation theory. However, such a simple picture no longer gives an accurate description when the population difference becomes large. The two-state model [15, 16, 17, 18, 19, 20] also reproduces the initial counterflow dynamics. However, since this model contains no mechanism for removing the system from the counterflow state, the two-state model predicts equilibration in a macroscopically quantum trapped state with larger population in the higher well. This inadequacy of the two-state model is based on the fact that it does not take higher lying modes into consideration [27].

Increasing the nonlinearity causes a reduction in the amount of initial counterflow,

and thus tends to inhibit the experimental observation. Fig. 3 illustrates the reduction in counterflow due to increased nonlinearity for fixed trap geometry, with \tilde{g} increasing by a factor of 10 from (a) to (c). This would appear to restrict the observation of the phenomenon to moderate nonlinearities (see next section for experimental estimates).

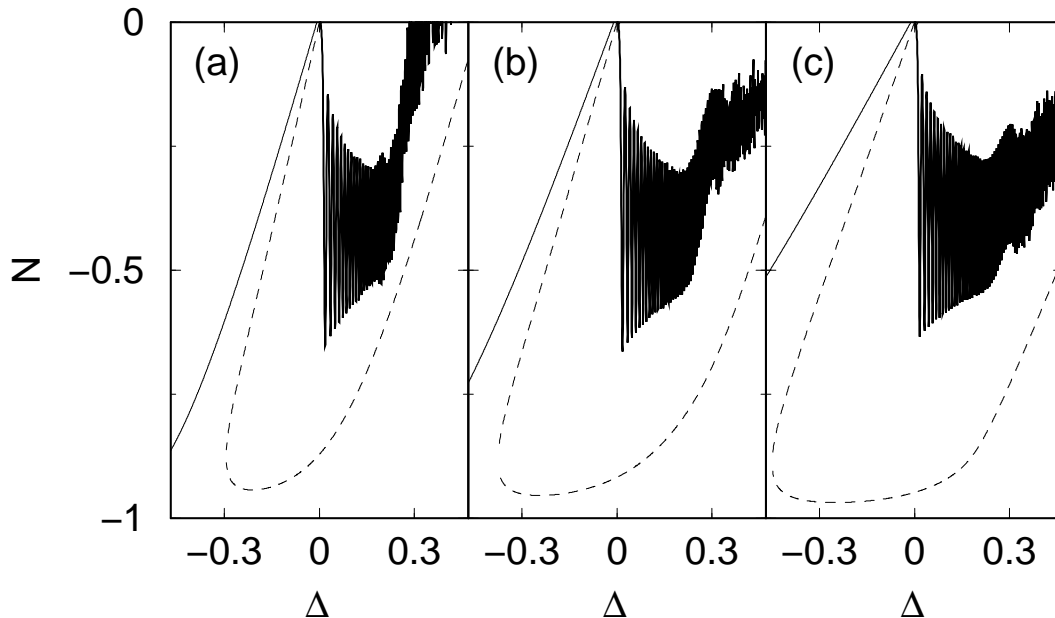


Figure 4. Dependence of fractional population difference dynamics on trap geometry. Plotted is the evolution of N as a function of potential gradient Δ for $R = 10^{-3}(\hbar\omega_{\perp}^2/a_{\perp})$ (black), $\tilde{g} = 10\pi$ and different trap aspect ratios: (a) cylindrically-symmetric trap $\lambda = 1$ ($h = 4\hbar\omega_{\perp}$) (same as Fig. 3(c)), (b)-(c) ‘pancake’-like traps with $\lambda = \sqrt{2}$ ($h = 6\hbar\omega_{\perp}$) and (c) $\lambda = \sqrt{8}$ ($h = 15\hbar\omega_{\perp}$), respectively. Note that larger barrier heights have been used with increasing aspect ratio, such that the density minimum at the trap centre is roughly constant from (a)-(c).

It is thus natural to ask if other factors (e.g. modifying initial trap aspect ratio, or changing barrier height h) will have the opposite effect on the amount of counterflow, hence enabling observation of Josephson counterflow even for large nonlinearities. For example, tunnelling has been predicted to be enhanced for ‘pancake’ traps ($\lambda > 1$) [24]. Indeed, for weak nonlinearities, such traps lead to a slightly increased counterflow amplitude. Furthermore, such geometries feature enhanced energy splitting between ground and first excited state, thus making them more robust to coupling due to external (e.g. thermal [18, 19, 48, 21]) perturbations. However, the reduction of the amplitude of counterflow due to increased nonlinearities tends to largely suppress this geometry dependence, as shown in Fig. 4 for trap aspect ratios in the range 1 to $\sqrt{8}$. In plotting this figure, the barrier height h has been increased for larger λ , such that the peak density in the trap centre remains essentially unchanged.

We should further comment on the extent to which our above findings depend on the rate R with which the linear potential gradient $\Delta = Rt$ is applied. The thick solid

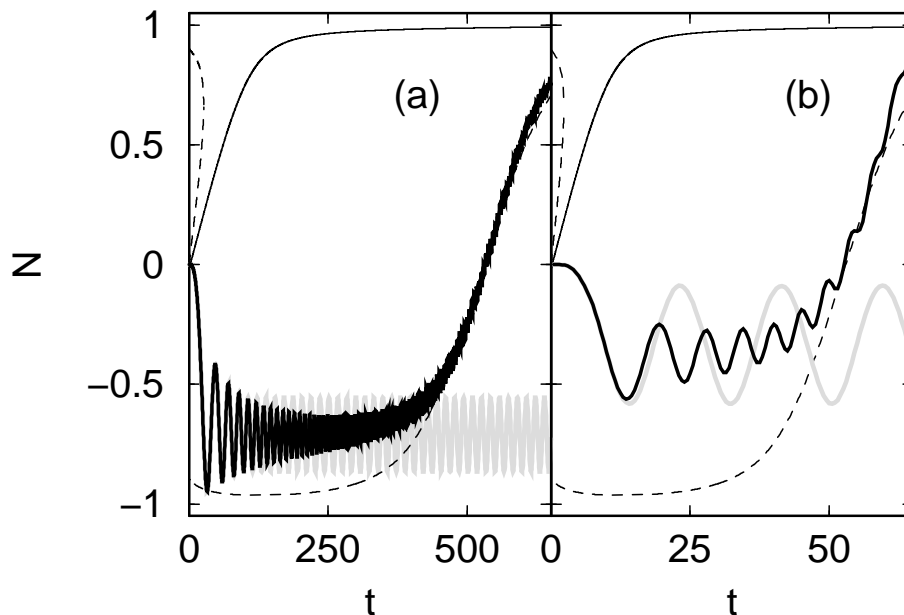


Figure 5. Evolution of fractional population difference N as a function of time (thick black lines) for different rates R of increase of the potential gradient: (a) $R = 10^{-3}(\hbar\omega_{\perp}^2/a_{\perp})$ and (b) $R = 10^{-2}(\hbar\omega_{\perp}^2/a_{\perp})$. Grey lines plot corresponding evolution of the population difference for the case when the potential gradient is held constant after a time $t =$ (a) $100\omega_{\perp}^{-1}$ and (b) $10\omega_{\perp}^{-1}$. Other parameters used, as in Fig. 3(a).

lines in Fig. 5 correspond to the evolution of the fractional population difference as a function of time. Fig. 5(a) shows the dependence for $R = 10^{-3}(\hbar\omega_{\perp}^2/a_{\perp})$ (as used in all earlier figures), whereas Fig. 5(b) shows the corresponding behaviour when the gradient is increased at a rate ten times faster than (a). One observes the following effects: firstly, the amount of maximum (initial) counterflow is significantly reduced (roughly by a factor of 2) by increasing the rate R by a factor of 10. Secondly, counterflow can only be observed for much shorter times (roughly reduced by a factor of 10).

A final question of interest is what would happen to the population difference if the applied linear potential is ramped up to a particular value and subsequently kept constant. The most striking behaviour will occur when the gradient is kept constant at the point of maximum population difference, as indicated by the grey lines in Fig. 5. We see that in this case, the population remains trapped in the right upper well, i.e. macroscopic quantum self-trapping occurs to a state with higher potential energy. In this regime, where the gradient does not exceed the value at which the flow is reversed, the two-state model predicts the behaviour correctly.

4. Experimental Considerations

Having demonstrated the existence of Josephson counterflow for a π -state initial wavefunction, we now discuss the feasibility of such observation in atomic BEC

experiments. Firstly, we need to discuss how such states with a node in the wavefunction and odd parity behaviour can be generated. Although not necessarily the most efficient method, here we consider phase imprinting [44]. Starting from the condensate ground state in a harmonic trap, population can be transferred to the first excited state by applying a light-induced potential of the form

$$V_r(z, t) = \alpha \sin(\pi t/\tau_0) \tanh(z) \quad (3)$$

for ($t < \tau_0$), where α and τ_0 are constants which we vary. This is equivalent to applying a π phase shift to the system. At $t = \tau_0$, the potential V_r is suddenly switched off, and the system exhibits Rabi oscillations of variable amplitudes and frequencies between the initial (ground) state and the first excited state. Fig. 6 shows fractional occupations ((a), (c)) and corresponding population differences ((b), (d)) for two different initial state preparation cycles. The fractional occupation of state i , denoting here ground (upper, thick solid) or first excited state (thin solid line), as a function of time, is given by

$$P(t) = |\langle \psi_i(z, t=0) | \psi(z, t) \rangle|^2. \quad (4)$$

This quantity measures excited population in any combination of the first excited states, and not only the population in the desired π -state. The subsequent Rabi oscillations are shown in Fig. 6(a). The corresponding atom number population difference between the two wells features π -oscillations (Fig. 6(b)) [39, 40], in which there is almost complete exchange of atoms between the two wells (i.e. essentially population exchange between the two macroscopically quantum self-trapped states of Fig. 1(c) (iii)). This phenomenon acts independently of the linear magnetic field gradient and tends to obscure the effect of Josephson counterflow. To demonstrate counterflow in its purest form, we thus consider the case (Fig. 6(c)) when the amplitude of such π -oscillations is suppressed (Fig. 6(d)), such that the majority of the population remains in the left, lower well at all times. Note that, in all cases studied here, the coupling with higher lying states is found to be negligible.

The importance of counterflow can be stressed, by first showing typical fractional population difference dynamics for a double well condensate in its *ground* state [27]. Application of the external potential at $t = 0$ creates a potential difference between the two wells, with flow occurring towards the lower well (located on the left for $\Delta > 0$). For the relatively slow rates of increase of the potential gradient studied here, the system follows the ground eigenstate almost adiabatically (Fig. 7(b)). In contrast, Figs. 7(c)-(d) show typical counterflow dynamics induced by the potential gradient $\Delta \neq 0$. This is based on the initial state preparation of Fig. 6(c)-(d) for $t \leq \tau_0$ and subsequent free evolution for $\tau_0 < t < \tau_1$ (as shown in Fig. 7(a)), with the potential gradient Δ applied at $t = \tau_1$. The evolution of the fractional population difference during this entire process is shown respectively by the solid lines in Fig. 7(c)-(d) for (c) $\tau_1 = 10\omega_{\perp}^{-1}$ and (d) $\tau_1 = 85\omega_{\perp}^{-1}$. The corresponding times when the potential gradient is applied are indicated by open circles in Fig. 7(a),(c)-(d). The effect of Josephson counterflow manifests itself clearly in that the population starts being transferred to the right, higher

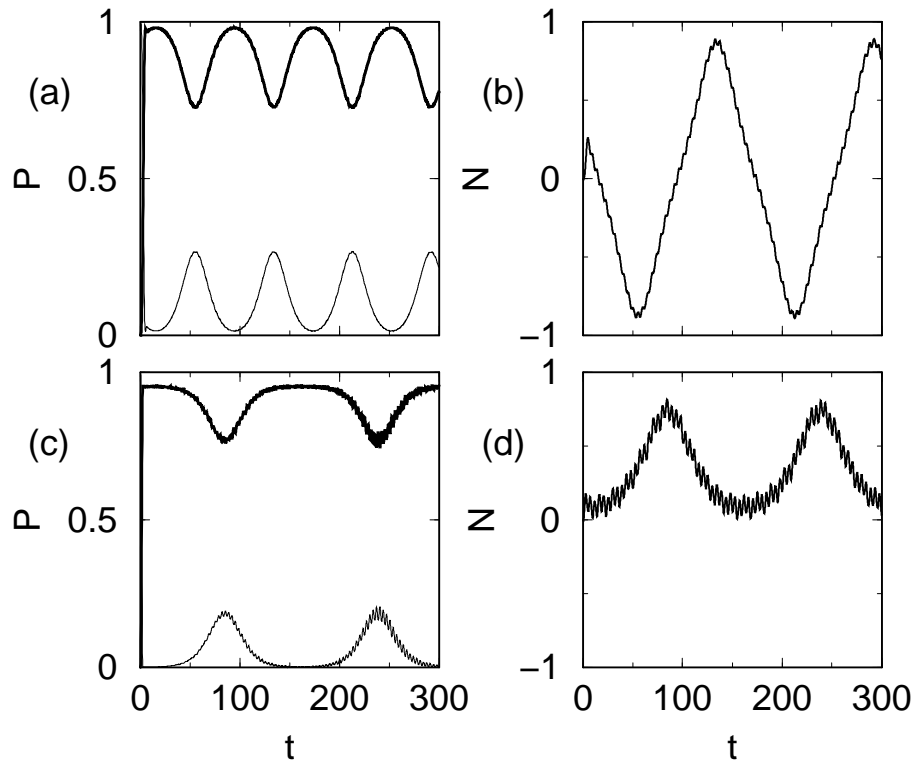


Figure 6. (a) Initial excited state preparation cycle and subsequent free evolution featuring Rabi oscillations ($\tau_0 = 6.5\omega_{\perp}^{-1}$, $\alpha = 0.5\hbar\omega_{\perp}$). (b) Corresponding fractional population differences, exhibiting π -oscillations. (c)-(d) Corresponding plots for different initial state preparation cycle ($\tau_0 = 3\omega_{\perp}^{-1}$, $\alpha = \hbar\omega_{\perp}$). In (d), the π -oscillations have been suppressed, with macroscopic quantum self-trapping occurring in the left, lower well. Other parameters as in Fig. 3(a).

potential energy well. Note that this is a direct consequence of the imposed magnetic field gradient (black curve), and that counterflow here occurs in a direction opposite to, and for larger amplitude than, the suppressed π -oscillations (grey lines). This indicates clearly the distinction between counterflow and π -oscillations.

We now look into typical experimental parameters which allow for demonstration of counterflow. In particular, we should investigate whether this effect is observable for an experimentally realistic number of atoms in the double-well condensate. The number of atoms is given by

$$\mathcal{N} = \frac{\tilde{g}}{4\pi} \frac{a_{\perp}}{a} = \frac{\tilde{g}}{4\pi a} \sqrt{\frac{\hbar}{m\omega_{\perp}}}. \quad (5)$$

It follows that, for given dimensionless nonlinearity \tilde{g} , large condensate atom number can be obtained for light, weakly-interacting, transversally weakly-confined systems. Note also that the total atom number is independent of the trap aspect ratio, as this cancels out for fixed \tilde{g} . Hence, for this effect to be observed clearly, with a large number of atoms, one should preferably choose atoms with a small value of $a\sqrt{m}$. This will hence yield large atom numbers for ${}^7\text{Li}$ and ${}^{23}\text{Na}$, with the corresponding numbers for ${}^{87}\text{Rb}$, ${}^{85}\text{Rb}$

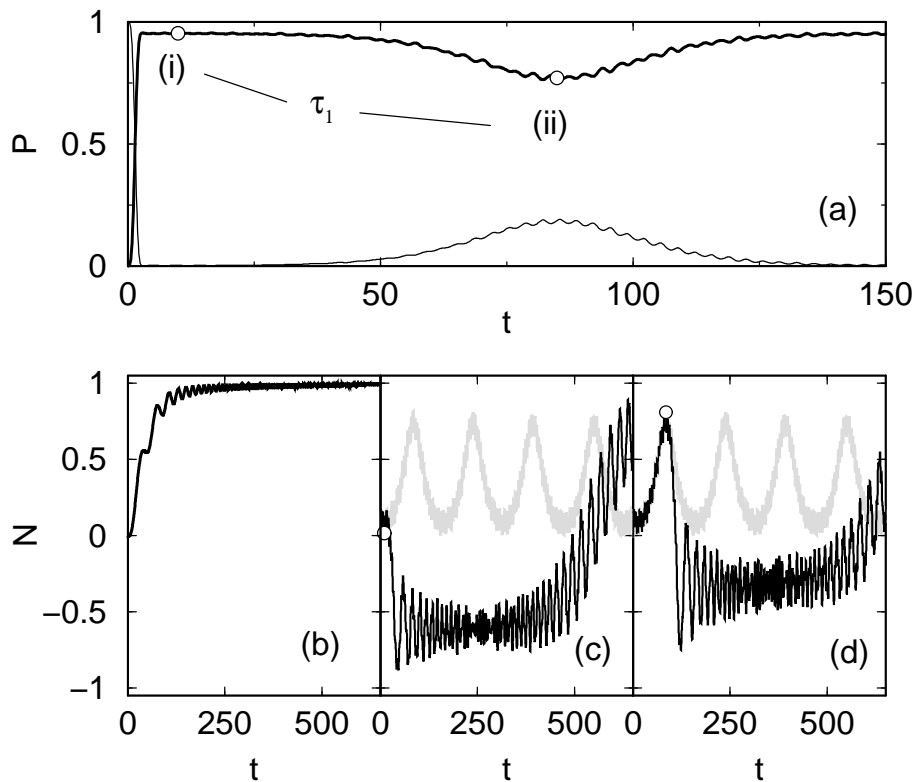


Figure 7. (a) Optimized π -state preparation cycle and subsequent free evolution featuring Rabi oscillations. (i) Maximum and (ii) minimum achievable efficiency of population transfer to first excited state ($\tau_0 = 3\omega_{\perp}^{-1}$, $\alpha = \hbar\omega_{\perp}$). (b)-(d) Evolution of fractional population difference N as a function of potential gradient Δ for different initial states: (b) Ground state condensate exhibiting usual Josephson flow towards lower (left) well, (c) Josephson counterflow (black) after efficient π -state preparation, induced by application of a potential gradient $\Delta = R(t - \tau_1)$ for $\tau_1 = 10\omega_{\perp}^{-1}$ (point (i) in Fig. (a)). Grey: corresponding evolution in the absence of the potential gradient, exhibiting (suppressed) π -oscillations. (d) Same as (c), but with $\tau_1 = 85\omega_{\perp}^{-1}$ (point (ii) in Fig. (a)). Other parameters as in Fig. 3(a).

considerably smaller. Nonetheless, this effect should be observable for all above species in experiments with resolution ability of detecting more than 1000 atoms. For example, taking $\tilde{g} = 4\pi$ as in Fig. 3(b) and $\omega_{\perp} = 2\pi \times 5$ Hz, we find the following atom numbers in the double well: $\mathcal{N} = 3300$ (^{23}Na) and 1000 (^{87}Rb). This number could be enhanced by a factor of 5 when using the nonlinearity of Fig. 3(c) and $\omega_{\perp} \sim 2\pi \times 1$ Hz, whereas further enhancement by a factor of 10 is possible by tuning around a Feshbach resonance (e.g. ^{23}Na , ^{85}Rb , ^{133}Cs [45]). In the case of ^7Li , this effect should be observable in a very clean manner, since in this case the constraint is placed on the maximum number of atoms which can be condensed such that it does not exceed the critical number leading to collapse [46]. In the case of ^{85}Rb , the number of atoms needed to observe Josephson counterflow is not likely to exceed the critical value for collapse. The effect of Josephson tunnelling on collapse will be investigated in subsequent work [47].

The possibility to demonstrate this effect experimentally will also depend on the timescales required for its observation. We consider the case of an applied magnetic field gradient $R = (10^{-3} - 10^{-2})(\hbar\omega_{\perp}/a_{\perp})$ and a typical transverse trapping frequency $\omega_{\perp} = 2\pi \times (5 - 100)\text{Hz}$. This translates into a magnetic field gradient inducing a Zeeman shift in the range $(1\text{MHz}-1\text{GHz})/\text{cm}$, and a dimensionless timescale of $\omega_{\perp}^{-1} = (32 - 1.6)\text{ms}$. Hence, for the illustrative parameters chosen here, efficient preparation of the π state requires a time $\tau_0 \sim (300 - 150)\text{ms}$. Observation of Josephson counterflow requires monitoring the population difference for at least a further time $t_{\text{exp}} \sim (1.5 \text{ s} - 75 \text{ ms})$. One notices two competing effects here: For fixed, reasonably small, nonlinearity ($\tilde{g} < 10\pi$), such that the effect can be clearly observed, one needs weak transverse confinement ω_{\perp} in order to obtain a reasonable number of atoms which can be imaged easily. Contrary to this, small ω_{\perp} imply long timescales, such that the observation of this effect becomes limited by other factors (e.g. thermal damping [18, 19, 48], 3-body recombination, etc.). The best conditions will hence depend on the details of each set-up, with reasonable parameters in the range $\omega_{\perp} \sim 2\pi \times (5 - 100)\text{Hz}$ and $\omega_z \sim 2\pi \times (1 - 500)\text{Hz}$, leading to total experimental timescales of $t_{\text{exp}} \sim 100 \text{ ms} - 2 \text{ s}$, and requiring an optimum resolution of a few hundred to a few thousand atoms.

5. Conclusions

We have studied the Josephson dynamics of a condensate in a double-well potential in the presence of a magnetic field gradient, for a suitably prepared initial antisymmetric state featuring equal populations in each well and a π -phase slip across the weak link. Under appropriate conditions, the atomic current was shown to flow in the direction opposite to that of minimum potential energy. This is the opposite behaviour to the ‘normal’ Josephson flow occurring for a system in its ground state. This phenomenon, termed here Josephson counterflow, bears close analogies to (metastable) π -states observed in superfluid- ^3He and (controllable) π -junctions in superconducting weak links. We have discussed a range of typical parameters for which this effect could be observed in atomic Bose-Einstein condensates. Observation of this effect in a ‘clean’ manner requires reasonably light, weakly-interacting atoms under rather weak transverse confinement, and techniques to populate the first excited state in a manner such that the π -oscillations are heavily suppressed. Optimum choice of parameters is an interplay between good experimental resolution for detecting few hundred to few thousand atoms, and the maximum observation time for which this effect is not affected by other dephasing processes. It is important to stress that appearance of this effect is not dependent on sign, and only weakly-dependent on strength of the scattering length, applying equally well to both attractive and repulsive Bose-Einstein condensates. An alternative suitable candidate for observing counterflow might also be found in the recently realized atom chips [49], which offer excellent control and experimental resolution. Investigation in these low dimensional systems should enable observation of Josephson counterflow, since we have found this effect to be only weakly dependent on aspect ratio of the harmonic

trap. We believe that the experimental observation of this phenomenon will further strengthen the analogies between atomic BEC's and other states exhibiting macroscopic phase coherence and controllable Josephson effects.

Acknowledgments

We acknowledge funding from the U.K. EPSRC.

- [1] Likharev 1979 Rev. Mod. Phys. **51** 101
- [2] Davis J C and Packard R E 2002 Rev. Mod. Phys. **74** 741
- [3] B. D. Josephson, Phys. Rev. Lett. **1**, 251 (1962)
- [4] Barone A and Paterno G *Physics and Applications of the Josephson Effect* (Wiley, New York, 1982).
- [5] Sukhatme K, Mukharsky Yu, Chul T and Pearson D 2001 Nature **411** 280
- [6] Avenel O and Varoquaux E 1988 Phys. Rev. Lett. **60** 416
 Pereverzev S V, Loshak A, Backhaus S, Davis J C and Packard R E 1997 Nature **388** 449
 Backhaus S, Pereverzev S V, Loshak A, Davis J C and Packard R E 1997 Science **278** 1435.
- [7] M. H. Anderson *et al.* 1995 Science **269** 198
 Davis K B et al 1995 Phys. Rev. Lett. **75** 3969
 Bradley C C et al 1997 Phys. Rev. Lett. **75** 1687
 Bradley C C et al. 1997 Phys. Rev. Lett. **79** 1170
 Fried D G et al. 1998 Phys. Rev. Lett. **81** 3811
 Robert A et al. 2001 Science **292** 461
 Dos Santos F P et al. 2001 Phys. Rev. Lett. **86** 3459
 Yosuke T, Maki K, Komori K, Takano T, Honda K, Kumakura M, Yabuzaki T and Takahashi Y
 2003 Phys. Rev. Lett. **91** 040404
- [8] Andrews M R, Townsend C G, Miesner H J, Durfee D S, Kurn D M and Ketterle W 1997 Science **275** 637
- [9] Shin Y, Leanhardt A E, Saba M, Pasquini T, Ketterle W and Pritchard D E 2003 Nature (subm.)
- [10] Tiecke T G, Kemmann M, Buggle Ch, Shvarchuck I, von Klitzing W and Walraven J T M 2003 J. Opt. B:Quantum Semiclass. Opt. **5** S119
- [11] Anderson B P and Kasevich M A 1998 Science **282** 1686
 Orzel C, Tuchman A K, Fenselau M L, Yasuda M and Kasevich M A 2001 Science **291** 2386
- [12] Cataliotti F S, Burger S, Fort C, Maddaloni P, Minardi F, Trombettoni A, Smerzi A, and Inguscio M 2001 Science **293** 843
- [13] Denschlag J H, Simsarian J E, Häffner H, McKenzie C, Browaeys A, Cho D, Helmerson K, Rolston S L and Phillips W D 2002 J. Phys. B: At. Mol. Opt. Phys. **35** 3095
- [14] Greiner M, Mandel O, Esslinger T, Hänsch T W and Bloch I 2002 Nature **415** 39
- [15] Jack M W, Collett M J and Walls D F 1996 Phys. Rev. A **54** R4625
- [16] Milburn G J, Corney J, Wright E M and Walls D F 1997 Phys. Rev. A **55** 4318
- [17] Smerzi A, Fantoni S, Giovanazzi S and Shenoy S R 1997 Phys. Rev. Lett. **79** 4950
- [18] Zapata I, Sols F and Leggett A 1998 Phys. Rev. A **57** R28
- [19] Javaneinen J and Ivanov M Yu 1999 Phys. Rev. A **60** 2351
- [20] Wu B and Niu Q 2000 Phys. Rev. A **61** 023402
- [21] Ruostekoski J and Walls D F 1998 Phys. Rev. A **58** R50
- [22] Williams J, Walser R, Cooper J, Cornell E and Holland M 1999 Phys. Rev. A **59**, R31
- [23] Salasnich L, Parola A and Reatto L 1999 Phys. Rev. A **60** 4171
- [24] Williams J 2001 Phys. Rev. A **64** 013610

- [25] Giovanazzi S, Smerzi A and Fantoni S 2000 Phys. Rev. Lett. **84** 4521
- [26] Menotti C, Anglin J R, Cirac J I and Zoller P 2001 Phys. Rev. A **63** 023601
- [27] Sakellari E, Leadbeater M, Kylstra N J and Adams C S 2002 Phys. Rev. A **66** 033612
- [28] Leggett A J and Sols F 1991 Found Phys **21** 353
- [29] Anglin J R, Drummond P and Smerzi A 2001 Phys. Rev. A **64** 063605
- [30] Zhou Y, Zhai H, Lu R, Xu Z and Chang L 2003 Phys. Rev. A **67** 043606
Li W-D, Zhang Yu and Liang J-Q 2003 Phys. Rev. A **67** 065601
- [31] Bulaevskii L N, Kuzii V V and Sobyenin A A 1977 JETP Lett. **25** 290
Geshkenbeim V B, Larkin A I and Barone A 1987 Phys. Rev. B **36** 235
- [32] van Harlingen D J 1995 Rev Mod Phys **67** 515
- [33] Ryazanov V V, Oboznov V A, Rusanov A Yu, Veretennikov A V, Golubov A A and Aarts J 2001 Phys. Rev. Lett. **86** 2427
- [34] Mühge Th et al 1996 Phys. Rev. Lett. **77** 1857
- [35] Baselmans J J A, Morpurgo A F, van Wees B J and Klapwijk T M 1999 Nature **397** 43
- [36] Baselmans J J A, van Wees B J and Klapwijk T M 2001 Appl. Phys. Lett. **79** 2940
- [37] Smilde H J H, Ariand, Blank D H A, Gerritsma G J, Hilgenkamp H and Rogalla H 2002 Phys. Rev. Lett. **88** 057004
- [38] Backhaus S, Pereverzev S, Simmonds R W, Loshak A, Davis J C and Packard R E 1998 Nature **392** 687
- [39] Marino I, Raghavan S, Fantoni S, Shenoy S R and Smerzi A 1999 Phys. Rev. A **60** 487
- [40] Raghavan S, Smerzi A, Fantoni S, and Shenoy S R 1999 Phys. Rev. A **59** 620
- [41] Raghavan S, Smerzi A and Kenkre V M 1999 Phys. Rev. A **60** R1787
- [42] H. Pu, L. O. Baksmaty, W. Zhang, N. P. Bigelow and P. Meystre, Phys. Rev. A **67**, 043605 (2003).
- [43] Wu B, Diener R B and Niu Q 2002 Phys. Rev. A **65** 025601
Diakonov D, Jensen L M, Pethick C J and Smith H 2002 Phys. Rev. A **66** 013604
Mueller E J 2002 Phys. Rev. A **66** 063603
- [44] Burger S et al. 1999 Phys. Rev. Lett. **83** 5198
Denschlag J et al. 2000 Science **287** 97
- [45] Inouye S, Andrews M R, Stenger J, Miesner H-J, Stamper-Kurn D M and Ketterle W 1998 Nature **392** 151
Roberts J L, Claussen N R, Cornish S L and Wieman C E 2000 Phys. Rev. Lett. **85** 728
Robert A et al. 2001 Science **292** 461
- [46] Bradley C C, Sackett C A and Hulet R G 1997 Phys. Rev. Lett. **78** 985
- [47] Sakellari E, Proukakis N P and Adams C S, 2003 In Preparation
- [48] Kohler S and Sols F 2003 New J. Phys. **5** 94
- [49] Ott H, Fortagh J, Schlotterbeck G, Grossmann A and Zimmermann C 2001 Phys. Rev. Lett. **87** 230401
Hänsel W, Hommelhoff P, Hänsch T W and Reichel J 2001 Nature **413** 498
Schneider S, Kasper A, vom Hagen Ch, Bartenstein M, Engeser B, Schumm T, Bar-Joseph I, Folman R, Feenstra L and Schiedmayer J 2003 Phys. Rev. A **67** 023612
Horak P, Klappauf B G, Haase A, Folman R, Schmiedmayer J, Domokos P and Hinds E A 2003 Phys. Rev. A **67** 043806